

Iron chelation-induced senescence-like growth arrest in hepatocyte cell lines: association of transforming growth factor β 1 (TGF- β 1)-mediated p27^{Kip1} expression

Gyesoon YOON¹, Hyun-Jung KIM, Young-Sil YOON, Hyeseong CHO, In K. LIM and Jae-Ho LEE

Department of Biochemistry and Molecular Biology, Ajou University School of Medicine, Wonchon-Dong, Paldal-Gu, Suwon 442-749, South Korea

Iron is essential for cellular proliferation in all organisms. When deprived of iron, the growth of cells is invariably inhibited. However, the mechanism involved remains largely unclear. In the present study, we have observed that subcytotoxic concentrations of desferrioxamine mesylate (DFO), an iron chelator, specifically inhibited the transition from G₁ to S-phase of Chang cells, a hepatocyte cell line. This was accompanied by the appearance of senescent biomarkers, such as enlarged and flattened cell morphology, senescence-associated β -galactosidase activity and reduced expression of poly(ADP-ribose) polymerase. Concomitantly, p27^{Kip1} (where Kip is kinase-inhibitory protein) was induced markedly, whereas other negative cell-cycle regulators, such as p21^{Cip1} (where Cip is cyclin-dependent kinase-interacting protein), p15^{INK4B} and p16^{INK4A} (where INK is inhibitors of cyclin-dependent kinase 4), were not, implying its association in

the G₁ arrest. Furthermore, the induction of p27^{Kip1} was accompanied by an increased level of transforming growth factor β 1 (TGF- β 1) mRNA. When neutralized with an anti-(TGF- β 1) antibody, p27^{Kip1} induction was completely abolished, indicating that TGF- β 1 is the major inducer of p27^{Kip1}. Finally, DFO-induced senescence-like arrest was found to be independent of p53, since cell-cycle arrest was still observed with two p53-negative cell lines, Huh7 and Hep3B cells. In conclusion, DFO induced senescence-like G₁ arrest in hepatocyte cell lines and this was associated with the induction of p27^{Kip1} through TGF- β 1, but was independent of p53.

Key words: desferrioxamine mesylate, Chang cells, G₁ arrest, p53.

INTRODUCTION

Iron is an essential element for the growth and maintenance of cells in all organisms. It participates in numerous critical biochemical processes, such as electron transfer for ATP synthesis in mitochondria, activation of ribonucleotide reductase (RR) for DNA synthesis, oxygen transfer by haemoglobin and activities of many other metalloenzymes [1–4]. In contrast with its essential role for cellular maintenance, an excess accumulation of iron can also raise serious health risks. Liver is a principal target organ for iron toxicity, because it functions to take up and store all the excess iron in the body. Heavy iron load has often been found in several liver diseases, including cirrhosis and hepatocellular carcinoma [5–10]. Therefore it has been suggested that the hepatic iron content, which results from its regulated uptake and availability, is closely associated with cellular proliferation and disorders in liver, regardless of their causes [11].

The proliferation ability of a cell is represented by a concerted modulation of cell-cycle progression. Transition from G₁ to S-phase basically progresses by catalytically active complexes composed of several different cyclins and cyclin-dependent kinases (CDKs), and is tightly controlled by CDK inhibitors (CDKIs). In mammalian cells, two families of CDKIs have been described on the basis of protein sequence similarity: the Cip/Kip (CDK-interacting protein/kinase-inhibitory protein) family, including p21^{Cip1} and p27^{Kip1}, and the INK (inhibitors of CDK4) family, including p16^{INK4A} and p15^{INK4B} [12,13]. Manipulation of cell-cycle progression by these CDKIs is a critical step in

determining the fate of cells to apoptosis, differentiation or senescence. ‘Replicative senescence’ is characterized by an irreversible state of cell-cycle arrest and is believed to play an important role in safeguarding against tumour formation by suppressing the emergence or growth of immortal cells [14,15]. Overexpression or induction of p53, p16^{INK4A} or p21^{Cip1} has been widely shown to cause premature senescence through G₁ arrest, indicating that these CDKIs and p53 are important mediators [16–18]. In contrast with the above, however, the involvement of p27^{Kip1} and p15^{INK4B} in cellular senescence is not well understood yet. A recent report [19] has described that senescence-like cell-cycle arrest by a phosphoinositide 3-kinase inhibitor was mediated through the accumulation of p27^{Kip1}, whereas p16^{INK4A}, p21^{Cip1}, p19^{ARF} (where ARF is alternative reading frame) and p53 were down-regulated. Activation of p15^{INK4B} has been observed only in senescent lymphocytes and was accompanied with an increase in p16^{INK4A} [20].

Cells deprived of iron do not proceed from G₁ to S-phase of the cell cycle and, therefore, iron chelation has often been employed to inhibit the growth of cancer cells. Indeed, desferrioxamine mesylate (DFO), a commonly used soluble iron chelator, has been shown to have anti-proliferative effects on a number of cell lines *in vitro*, including hepatoma, leukaemia and neuroblastoma cells [21–24]. Moreover, in several *in vivo* trials using nude mice and rats, DFO was found to decrease the incidence of cancer development [25,26]. Despite various studies on growth inhibitory effects of DFO, its detailed molecular mechanism is poorly understood. Recently, we found that

Abbreviations used: BrdU, 5-bromo-2'-deoxyuridine; CDK, cyclin-dependent kinases; CDKI, cyclin-dependent kinase inhibitors; Cip/Kip, CDK-interacting protein/kinase-inhibitory protein; DAPI, 4,6-diamidino-2-phenylindole; DFO, desferrioxamine mesylate; DMEM, Dulbecco's modified Eagle's medium; FBS, fetal bovine serum; GAPDH, glyceraldehyde-3-phosphate dehydrogenase; INK, inhibitors of CDK4; PI, propidium iodide; PARP, poly(ADP-ribose) polymerase; RR, ribonucleotide reductase; RT, reverse transcriptase; SA- β -gal, senescence-associated β -galactosidase; TGF- β 1, transforming growth factor β 1.

¹ To whom correspondence should be addressed (e-mail ypeace@madang.ajou.ac.kr).

treatment of Chang cells, an immortalized human hepatocyte cell line, with subcytotoxic concentrations of DFO induced enlarged and flattened cellular morphology (G. Yoon, H.-J. Kim, Y.-S. Yoon, H. Cho and J.-H. Lee, unpublished work), which is one of the typical characteristics of cellular senescence. This phenotype appeared within 3 days and lasted up to 10 days, and was irreversible. In the present study, we have explored the mechanism involved in the senescence-like growth arrest of hepatocyte cell lines induced by DFO. We conclude that DFO induced senescence-like G_1 arrest in hepatocyte cell lines and the arrest was associated with p27^{Kip1} induction through transforming growth factor $\beta 1$ (TGF- $\beta 1$) expression, but was independent of p53.

MATERIALS AND METHODS

Cell culture and growth curves

Chang cells were cultured in Dulbecco's modified Eagle's medium (DMEM) containing F-12 nutrient mixture (1:1, v/v; DMEM/F12; Gibco BRL, Gaithersburg, MD, U.S.A.) and 10% (v/v) fetal bovine serum (FBS; Gibco BRL) in a 37 °C incubator with 5% CO₂ in air. Hep3B and Huh7 cells were cultured in DMEM (Gibco BRL) containing 10% FBS. Growth rates of DFO-treated Chang cells were monitored by counting the viable cells. Briefly, 1×10^3 cells were seeded into 24-well plates, cultured in DMEM/F12 containing 10% (v/v) FBS for 12 h, and treated with various concentrations of DFO for the indicated periods. The cells were kept in culture by refreshing with DMEM/F12 and 10% (v/v) FBS containing DFO every 3 days. At the indicated times, cells were harvested by trypsinization and counted with a haemocytometer after staining with 0.4% (w/v) Trypan Blue (Gibco BRL) to exclude dead cells.

Proliferation rate by 5-bromo-2'-deoxyuridine (BrdU) incorporation assay

The proliferation rate was analysed by counting the number of cells incorporating BrdU and comparing with the total number of cells stained with 4,6-diamidino-2-phenylindole (DAPI), according to the manufacturer's instructions (BrdU incorporation assay kit; Boehringer Mannheim, Mannheim, Germany), with a slight modification. Subconfluent cells were seeded on to coverslips and treated in the absence or presence of DFO (500 μ M) for the indicated periods. Cells were then labelled with 20 μ M BrdU in DMEM/F12 containing 10% (v/v) FBS for 4 h to increase BrdU incorporation. The cells were fixed with 70% (v/v) ethanol in 50 mM glycine buffer (pH 2.0) for 20 min. The labelled cells were visualized by incubating with an anti-(BrdU) antibody and Cy3-conjugated anti-(mouse IgG) antibody. Co-staining with DAPI was applied to visualize total cells.

Cell-cycle analysis

Cell-cycle analysis was performed by propidium iodide (PI) staining according to the protocol provided with CycleTEST™ PLUS DNA reagent kit (Becton Dickinson, Mississauga, ON, Canada). Subconfluent cells treated in the absence or presence of DFO for the indicated periods were trypsinized, collected by centrifugation, and washed with, and resuspended in, PBS before fixing in 70% (v/v) ethanol at a density of 1×10^6 cells/ml. After RNase digestion (0.1 mg of RNase A and 2 units/ml of RNase T1 at 37 °C for 1 h) and washing with PBS, the fixed cells were stained with 50 μ g/ml PI for at least 30 min before analysis by

flow cytometry (FACSorter; Becton Dickinson). The instrument was set to collect 2×10^4 cells and the cell-cycle profile was analysed using CellQuest software.

Senescence-associated β -galactosidase (SA- β -gal) assay

SA- β -gal was assayed at pH 6.0 as described by Dimri et al. [27] with a slight modification. Briefly, cells were washed twice with PBS, fixed to plates by 3% formaldehyde for 5 min, washed with PBS, and then incubated overnight in freshly prepared staining solution [40 mM citrate/phosphate buffer (pH 6.0) containing 1 mg/ml 5-bromo-4-chloroindol-3-yl β -D-galactopyranoside ('X-Gal'; Sigma, St. Louis, MO, U.S.A.), 5 mM potassium ferrocyanide, 5 mM potassium ferricyanide, 150 mM NaCl and 2 mM MgCl₂]. The stain was visible 12 h after incubation at 37 °C. The degree of senescence-associated cells was obtained by counting the number of blue-stained cells per field (0.5 cm \times 0.5 cm) and expressing as a percentage of the total number of cells.

Neutralization of the TGF- $\beta 1$ with an anti-(TGF- $\beta 1$) antibody

Subconfluent Chang cells were cultured for 12 h, and then treated with 1 mM DFO. TGF- $\beta 1$ released from the DFO-treated Chang cells was neutralized by adding a specific anti-(TGF- $\beta 1$) antibody (MAB240; R & D Systems, Minneapolis, MN, U.S.A.) immediately or 1 day after DFO treatment. The media containing the neutralizing antibody was replaced everyday for the indicated period of time in presence of 1 mM DFO.

Western-blot analysis and antibodies

Cells were washed twice with PBS and lysed with lysis buffer [50 mM Tris/HCl (pH 7.5), 0.1 M NaCl, 1 mM EDTA, 1% (v/v) Triton X-100, 10 μ g/ml each of aprotinin and leupeptin, and 1 mM PMSF]. A portion (40 μ g) of the lysate was separated by SDS/PAGE, and the proteins were electrically transferred on to a nitrocellulose membrane (Protran; Schleicher and Schuell, Keene, NH, U.S.A.). The membrane was blocked for 1 h at 24 °C with blocking solution [PBS containing 0.05% Tween 20 (PBST) and 5% (w/v) non-fat milk]. Subsequently, the membranes were incubated in blocking solution at 4 °C with 1 μ g/ml of antibodies against p27^{Kip1} (clone 57; Transduction Laboratories, Lexington, KY, U.S.A.), p21^{Cip1} (C-17; Santa Cruz Biotechnology, Santa Cruz, CA, U.S.A.), p53 (DO-1; Santa Cruz Biotechnology), p16^{INK4A} (G175-1239; BD PharMingen, San Jose, CA, U.S.A.), p15^{INK4B} (MCA1988; Serotec, Kidlington, Oxford, U.K.), poly(ADP-ribose) polymerase (PARP; C2-10; Zymed Laboratories, San Francisco, CA, U.S.A.), caspase 3 (SC-7272, Santa Cruz Biotechnology) or phospho-p53 (phospho-p53 antibody sampler kit; Cell Signaling Technologies, Beverly, MA, U.S.A.). Membranes were then washed twice with PBST, incubated with horseradish peroxidase-conjugated goat anti-(rabbit IgG) or anti-(mouse IgG) antibodies (Amersham Biosciences, Piscataway, NJ, U.S.A.) for 1 h at 24 °C. Detection was determined by treating the membranes with enhanced chemiluminescence reagents (ECL®; Amersham Biosciences) and exposing to X-ray film.

Reverse transcriptase (RT)-PCR

Total RNA was prepared by using the guanidium method [28], and cDNA was obtained by incubating 0.5 μ g of total RNA with 50 pmol of oligo(dT) primer and 0.25 unit of AMV ('Avian Myeloblastosis Virus') RT XL in a 20 μ l reaction mixture (RNA

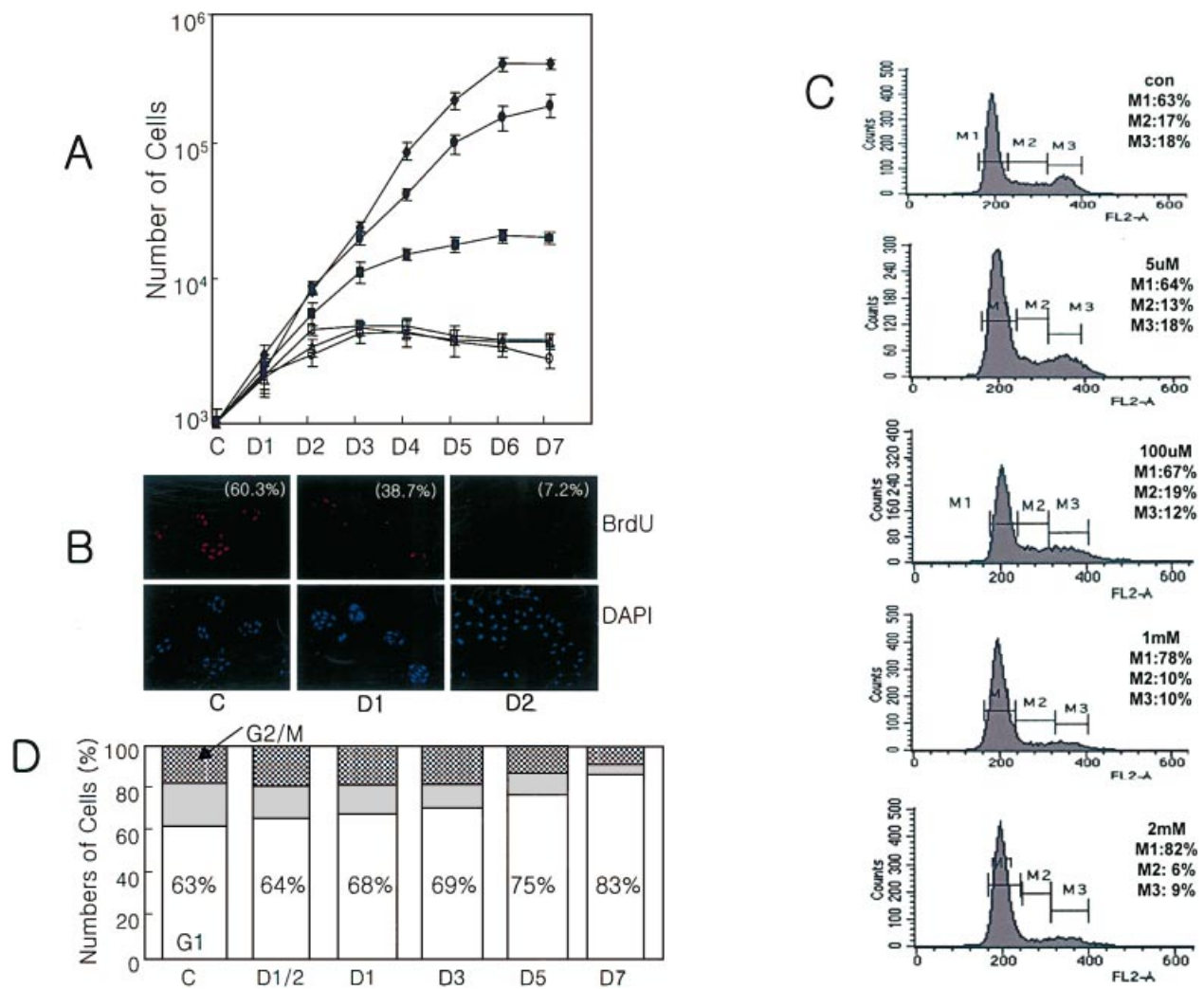


Figure 1 Dose-dependent growth arrest by DFO at G₁ phase of the cell cycle in Chang cells

(A) Logarithmically growing Chang cells (1×10^3) were seeded into 24-well plates and cultured in DMEM/F12 containing 10% (v/v) FBS for 12 h, and treated in the absence (\blacklozenge) or presence of 5 μM (\bullet), 20 μM (\blacksquare), 100 μM (\square), 1 mM (\triangle) or 2 mM (\circ) DFO for the indicated periods. At the indicated times, cells were harvested by trypsinization and counted by excluding dead cells with Trypan Blue staining. Results are means \pm S.D. from four independent experiments. (B) The proliferation rate was analysed by BrdU incorporation assay as described in the Materials and methods section. The number in each panel represents the mean percentage of BrdU-incorporated cells compared with the total number of cells as determined by DAPI-stained cells [control (C), $60.3 \pm 5.9\%$; 1 day (D1) of DFO treatment, $38.7 \pm 5.1\%$; and 2 days (D2) of DFO treatment, $7.2 \pm 1.7\%$; means \pm S.D. of triplicate observations]. A representative experiment is shown. (C) Subconfluent cells (1×10^6) were cultured for 3 days in the absence (con) or presence of the indicated concentrations of DFO. The cells were collected by trypsinization and stained with PI prior to flow cytometric analysis. M1, M2 and M3 represent G₁, S- and G₂/M phases of the cell cycle respectively. A representative result from two independent experiments is shown. (D) Time-dependent cell-cycle arrest was analysed by flow cytometric analysis. Subconfluent cells (1×10^6) were treated with 1 mM DFO for the indicated time periods and then harvested and stained with PI. The numbers in the open bars indicate the mean percentage of the cells arrested in G₁ phase [control (C), $63.1 \pm 2.1\%$; 12 h (D1/2), $64.3 \pm 0.7\%$; 1 day (D1), $68.3 \pm 2.8\%$; 3 days (D3), $69.2 \pm 2.2\%$; 5 days (D5), $75.2 \pm 1.6\%$; and 7 days (D7), $83.3 \pm 2.1\%$; means \pm S.D. of three independent experiments]. The percentages of the cells in S- and G₂/M phases are represented by closed and stippled bars respectively. C, cells at day 0; D, number of days of DFO treatment.

PCR kit version 2.1; TaKaRa, Shiga, Japan) at 30 °C for 10 min, 56 °C for 30 min, and then 90 °C. A portion (100 ng) of the TGF- β 1 primers (5'-GCCCTGGACACCAACTATT-3' and 5'-TCAGCTGCACTTGCAGGAG-3', with the PCR product spanning from exons 5–7) and 50 ng of the glyceraldehyde-3-phosphate dehydrogenase (GAPDH) primers (5'-CCATGGAGAAGGCTGGGG-3' and 5'-CAAAGTTGTCATGGATGACC-3') were added to give a final volume of 100 μl in a single reaction mixture with 1 unit of Ex *Taq* polymerase (TaKaRa). PCR conditions were: denaturation at 94 °C for 30 s, annealing at 50 °C for 30 s, and elongation at 72 °C for 30 s. Serial PCR products from 25–32 cycles were screened. The final RT-

PCR products were electrophoresed on 1.2% (w/v) agarose gels, stained with 0.5 $\mu\text{g}/\text{ml}$ of ethidium bromide solution, and visualized on a UV transilluminator.

RESULTS

DFO arrests the growth of Chang cells at G₁ phase in a dose-dependent manner

Exponentially growing asynchronous Chang cells, immortalized normal human hepatocytes, were treated with various concentrations of DFO, a water-soluble iron chelator, and the growth

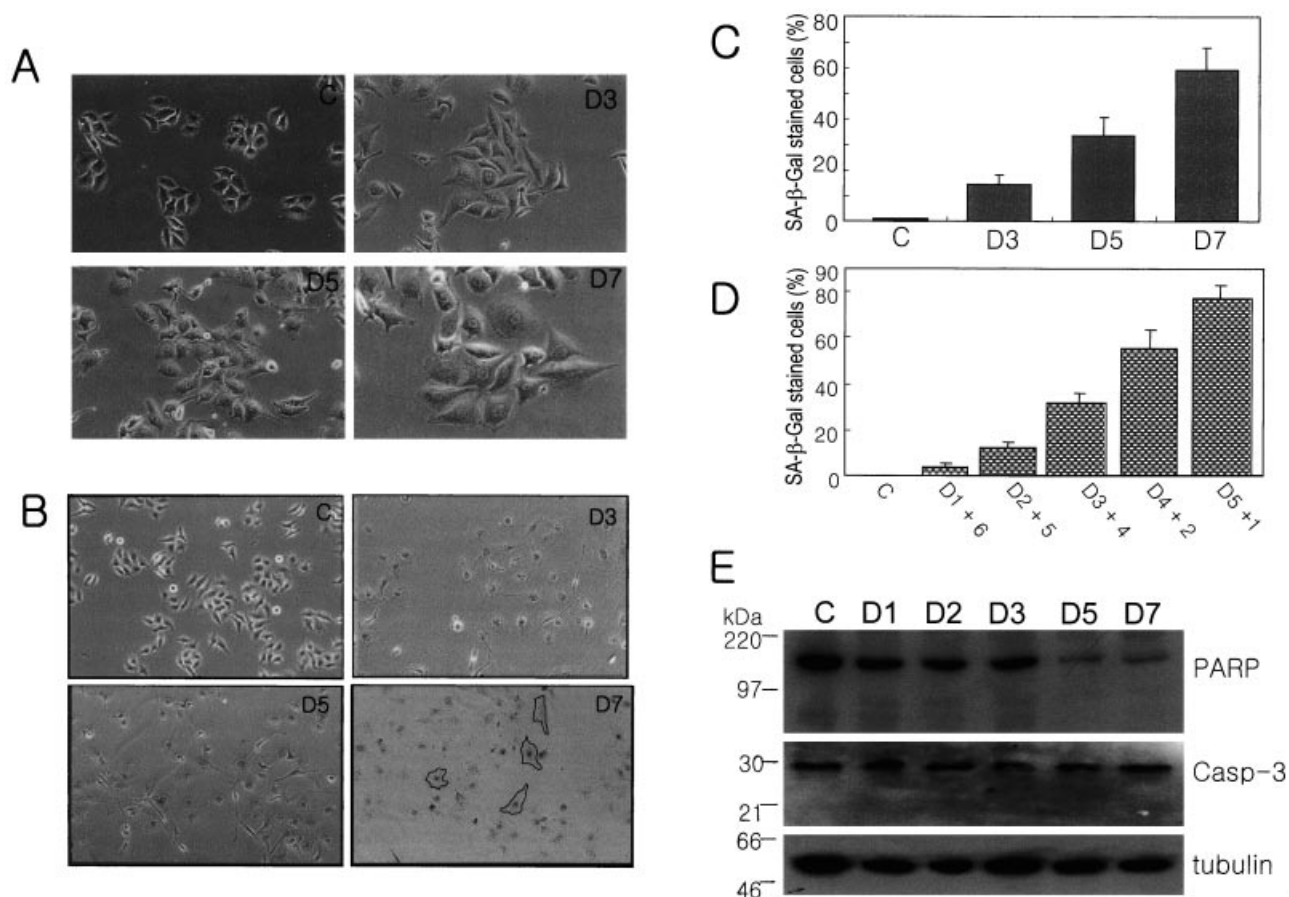


Figure 2 Gain of SA- β -gal activity, morphological changes and decrease of PARP expression by DFO represent senescence-like arrest

Chang cells (2×10^5) were seeded into 6-well plates, cultured for 12 h in DMEM/F12 containing 10% (v/v) FBS, and treated in the absence or presence of 1 mM DFO for the indicated periods. Every 3 days, the media was replaced with or without DFO and, if necessary, the cells were passaged to keep subconfluent. (A) Cellular morphology of Chang cells at 3 (D3), 5 (D5) and 7 (D7) days after treatment with 1 mM DFO compared with that of untreated cells. Magnification, $\times 140$. (B) Cells after 3 (D3), 5 (D5) and 7 (D7) days of treatment with 1 mM DFO were stained for SA- β -gal activities. The boundaries of a number of cells at day 7 are marked to visualize the cell size. Magnification, $\times 70$. (C) Strongly stained cells with SA- β -gal activity were counted and expressed as a percentage of the total number of cells, as described in the Material and methods section. Results are means \pm S.D. of five fields. (D) Effect of duration of DFO treatment on SA- β -gal activity. Chang cells were treated with 1 mM DFO for a various periods of time (D), the media was removed and replaced with media without DFO for remaining number of days (+n). The SA- β -gal activity was examined on day 8. Results are means \pm S.D. of five fields. (E) Western-blot analysis for PARP and caspase-3 expression. Representative blots from three independent experiments are shown. The number of days (D) after DFO treatment are indicated. Molecular-mass markers (in kDa) are shown on the left. C, untreated cells.

rate of the cells was monitored by counting the viable cells over the time course of treatment. The growth curves (Figure 1A) show that there was a significant decline in growth rates of the DFO-treated cells in a dose-dependent manner. With DFO concentrations higher than $100 \mu\text{M}$, almost complete growth arrest was evident after 48 h. No significant number of dead cells was observed until 4 days of DFO treatment, as judged by floating cells during culture or Trypan Blue-stained cells (results not shown). A number of dead cells appeared after 4 days of treatment with DFO concentrations higher than $100 \mu\text{M}$, resulting in a slight decline of the growth curve. Next, using the BrdU incorporation assay, we examined further whether the growth arrest was caused by the inhibition of proliferation rate. As shown in Figure 1(B), the percentage of BrdU-incorporated cells was clearly decreased from $60.3 \pm 5.9\%$ (control; mean \pm S.D.) to $7.2 \pm 1.7\%$ (mean \pm S.D.) after 2 days of exposure to DFO, and few weakly labelled cells (0–2%) were observed after the third day. It was therefore obvious that the initial growth arrest by DFO was due to a decreased proliferation rate.

In contrast with the low concentrations required for effective growth arrest in neuroblastoma, where 1–10 μM decreased the cell number by 50% with massive apoptotic cell death after 24 h of exposure [24], relatively higher concentrations (higher than 2 mM) were needed to induce apoptotic death in Chang cells. This difference could be due to the fact that liver is an iron-storage organ with much higher tolerance towards iron depletion than other organs, or that hepatocytes may have another hitherto unknown protective mechanism against iron depletion.

To analyse further the effect of DFO on the cell cycle, flow cytometric analyses with PI staining were performed. As shown in Figure 1(C), cells in G_1 phase increased from 63% (control) to 78% (1 mM) and 82% (2 mM) after 3 days of exposure with DFO. The number of cells arrested at the G_1 phase also increased in a time-dependent manner, with 83% after 7 days of exposure to 1 mM DFO (Figure 1D). Our data therefore demonstrate that the growth inhibition of Chang cells by DFO was caused primarily by arrest at the G_1 phase of the cell cycle in a dose- and time-dependent manner.

Irreversible senescence-like change of Chang cells by DFO

During the growth arrest by DFO, we observed that Chang cells progressively displayed enlarged morphology mimicking replicative-senescent cells. It is generally accepted that replicative-senescent cells display flat cell morphology, are irreversibly arrested during the G₁ phase of cell cycle, have increased expression of p16^{INK4a}, p21^{Cip1} and p19^{ARF} (where ARF is alternative reading frame), enhanced p53 activity and reduced PARP expression [14–18,29]. To confirm whether DFO induced cellular senescence in Chang cells, first we examined microscopic morphological changes. Chang cells started to manifest enlarged and flattened cell morphology within 24 h after treatment with 1 mM DFO and their size progressively increased until 7 days of treatment (Figure 2A). Another widely used marker for cellular senescence is the acquisition of SA- β -gal activity [27], and DFO-treated Chang cells clearly induced SA- β -gal activity (Figures 2B and 2C). The proportion of SA- β -gal-stained cells increased as the exposure time increased, with 14.3% of the total cells after exposure for 3 days with 1 mM DFO, 33.7% after 5 days, and 59.3% after 7 days of treatment (Figures 2B and 2C). Dose-dependent SA- β -gal activation was also observed (results not shown). We therefore decided to use 1 mM DFO to analyse the molecular mechanism involved, because of its intermediate, but evident, effect on both growth arrest and acquisition of the senescent phenotype.

To explore the irreversibility of the senescence-like property, Chang cells were treated with 1 mM DFO for various periods of time prior to the culture medium being replaced with medium lacking DFO. Transient exposure of the cells to DFO for at least 1 day induced a small proportion of the cells to exhibit SA- β -gal activity, and the proportion of SA- β -gal-stained cells increased as the exposure time was increased (Figure 2D). Moreover, the number of stained cells was higher in cells that were exposed to DFO for 3 days followed by normal media for 3 days (Figure 2D, bar 4) than those exposed to DFO for 3 days only (Figure 2C, bar 2). This result suggested that, once stimulated by DFO, the cells kept progressing to senescence even in the absence of DFO, and that the senescence-like characteristic induced by DFO was irreversible. To confirm further the senescent characteristic induced by DFO, expression of PARP was monitored by Western-blot analysis. PARP has been shown to limit the extent of DNA damage-induced genomic instability and to decrease in expression during cellular senescence, thus possessing a role as a senescent marker [29–31]. As shown in Figure 2(E), PARP expression in Chang cells started to decrease after 3 days of exposure to DFO without any appearance of the 89 kDa fragmented PARP, as detected by an anti-(PARP) antibody that detects both the full-length and fragmented PARP. To prove further that the decrease in PARP was not caused by cleavage by activated caspase-3, the expression level of caspase-3 was also analysed. No decrease in the level of procaspase-3 expression was observed, indicating that caspase-3 was not activated. These results imply that genomic stability might have been decreased during the DFO-induced genotoxic stress condition. Taken together, it can be summarized at this point that the G₁ arrest induced by DFO is accompanied by a dose-dependent senescence-like change in the cells.

Growth arrest by DFO associated with induction of p27, but not of p21

Several reports [14–18,32,33] have indicated that cellular senescence is induced by the overexpression of p16^{INK4A}, p21^{Cip1} or p53, implying their roles as major mediators in the senescent process. To test this possibility, the expression of p53 was

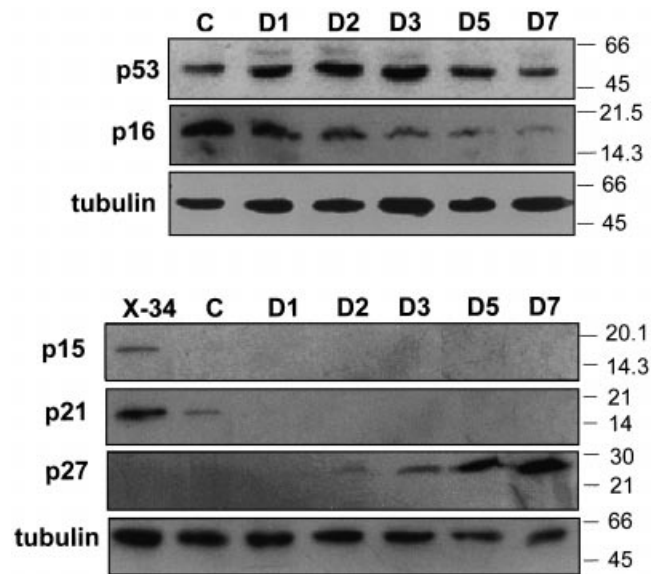


Figure 3 G₁ arrest by DFO mediated through induction of p27^{Kip1}, but not of p21^{Cip1}

Time-dependent expression of p53 and CDKIs, including p15^{INK4b} (p15), p16^{INK4a} (p16), p21^{Cip1} (p21) and p27^{Kip1} (p27), were examined by Western-blot analysis. X-34 represents a cell lysate obtained from Chang cells overexpressing the X protein of Hepatitis B virus and used as a positive control. The levels of tubulin were used as a protein-loading control. Representative blots from three independent experiments are shown. The number of days (D) after DFO treatment are indicated. Molecular-mass markers (in kDa) are indicated on the right. C, untreated cell lysate.

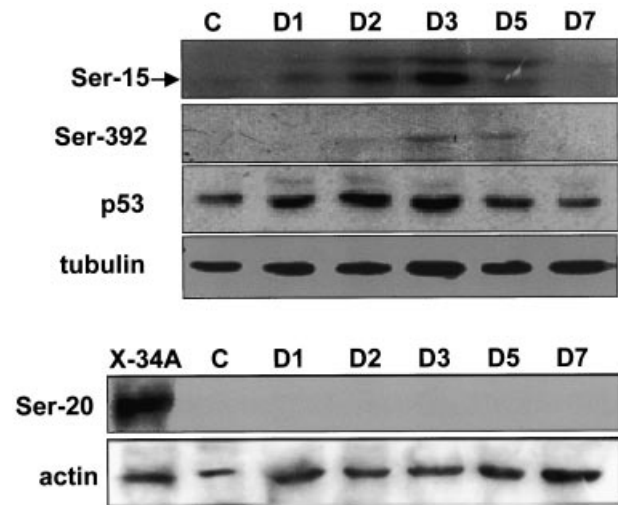


Figure 4 Differential phosphorylation level on various phosphorylation sites of p53

Time-dependent phosphorylation of p53 on Ser-15, Ser-20 and Ser-392 was examined by Western-blot analysis using specific antibodies against each phosphorylated residue of p53. X-34A, adriamycin-treated X-34 cell lysate was used as positive control for detection of Ser-20 phosphorylation. Representative blots from three independent experiments are shown.

examined by Western-blot analysis. As shown in Figure 3, p53 protein expression increased progressively until day 3 of DFO treatment, and then slowly returned back to control levels. However, p21^{Cip1}, a downstream target protein of p53, was not

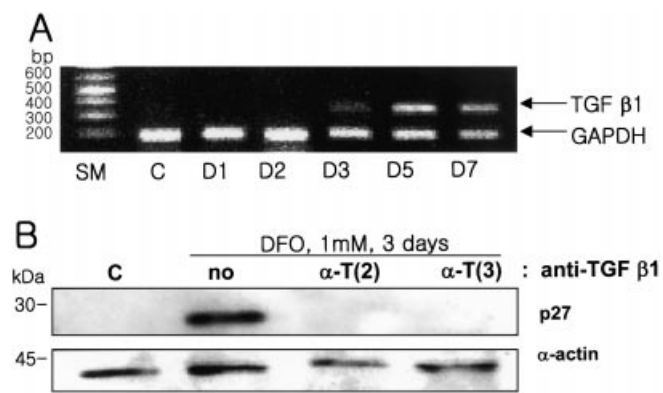


Figure 5 Induction of p27^{Kip1} expression and its effect on growth arrest mediated by TGF- β 1

(A) Transcriptional induction of TGF- β 1 was examined by RT-PCR as described in the Materials and methods section. The positions of TGF- β 1 and GAPDH are indicated. Lane SM shows a 100 bp ladder. Each lane is labelled as in Figure 2(E). (B) Subconfluent Chang cells were cultured for 12 h and then treated with 1 mM DFO for 3 days in the absence (no) or presence of the neutralizing anti-(TGF- β 1) antibody (2 μ g/ml) applied immediately after DFO treatment. The medium containing the anti-(TGF- β 1) antibody was replaced every day for two [α -T(2)] or three [α -T(3)] days. Following treatment, the expression of p27^{Kip1} was analysed by Western blotting. The levels of α -actin were used as a protein-loading control. Molecular-mass markers (in kDa) are indicated on the left. Representative blots from three independent experiments are shown.

induced, indicating that the increased level of p53 protein did not play a role as the transcriptional activator of p21^{Cip1} expression. This result encouraged us to screen the regulators involved in G₁ arrest, and the expression levels of CDKIs, including p16^{INK4A}, p15^{INK4B} and p27^{Kip1}, were analysed by immunoblotting. Neither p16^{INK4A} nor p15^{INK4B} were accumulated, whereas the level of p16^{INK4A} and p21^{Cip1} decreased. However, there was an obvious induction of p27^{Kip1} after exposure for 3 days, and its induction continued to increase thereafter. These findings suggested that the induction of p27^{Kip1} might play a role as a mediator of this cell-cycle arrest.

Next, we asked why the increased p53 did not induce p21^{Cip1}. Recent studies [34–36] have shown that differential phosphorylation on various sites of p53 can modulate its stability as well as induction of its downstream gene products. Therefore we examined the level of phosphorylation of each phosphorylation site of p53 by using antibodies which specifically recognize a particular phosphorylated residue of the p53 protein. As shown in Figure 4, phosphorylation of Ser-15 increased proportionately with the increase in p53 expression, whereas no phosphorylation of Ser-20 was detected. A slight transient increase in phosphorylation of Ser-392 was observed. These observations possibly indicate that markedly enhanced phosphorylation of Ser-15, but with no phosphorylation of Ser-20, blocked the p21^{Cip1} induction by p53, findings consistent with a previous report [35].

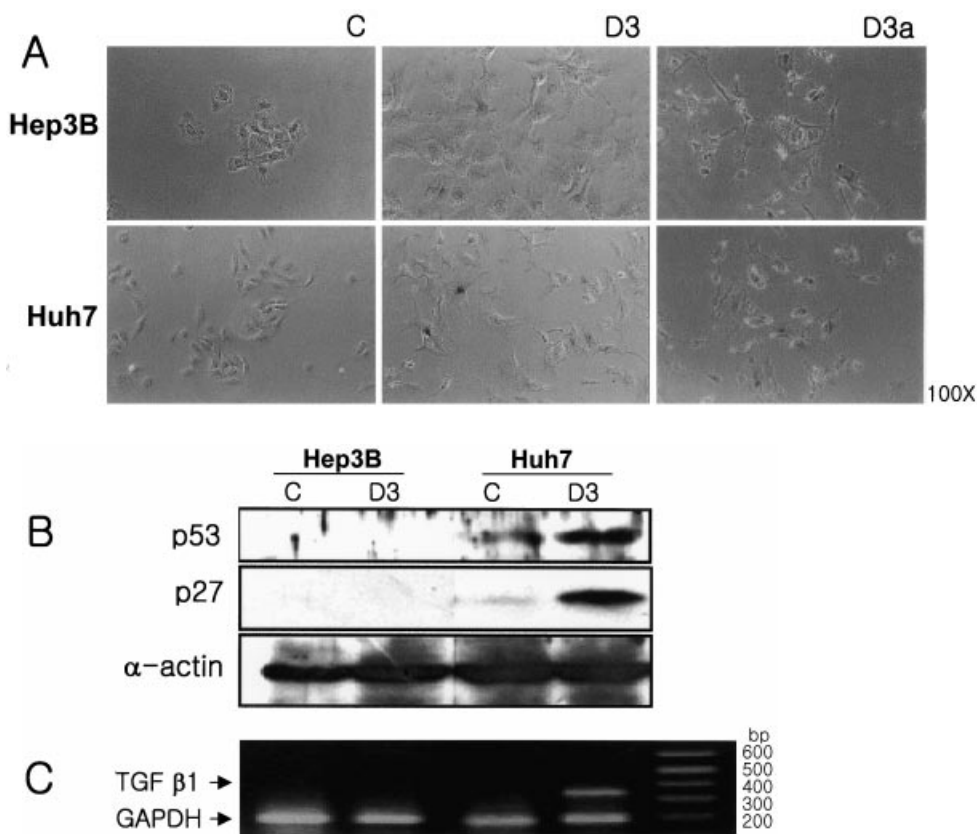


Figure 6 Senescence-like growth arrest by iron chelation independent of p53

Hep3B and Huh7 cells were treated in the absence (C) or presence (D3) of DFO for 3 days. (A) Cells were stained to assess SA- β -gal activity. To intensify the staining with 5-bromo-4-chloroindol-3-yl β -D-galactopyranoside, the incubation time was increased to 48 h (D3a). Lane SM shows a 100 bp ladder. Magnification, \times 65. (B) Protein expression of p53 and p27^{Kip1} following treatment was determined by Western blotting. (C) mRNA levels of TGF- α 1 and GAPDH in Hep3B and Huh7 cells was determined by RT-PCR. The lanes correspond to those shown in (B). A 100 bp ladder is shown on the right. Representative blots from three independent experiments are shown.

Induction of p27 expression mediated by transcriptional induction of TGF- β 1

So far, the results described above suggested that the up-regulation of p27^{Kip1} expression was associated in DFO-induced senescence-like G₁ arrest in Chang cells. We therefore attempted to explore possible factors in the induction of p27^{Kip1} expression. Since several previous reports [37,38] have described that p27^{Kip1} expression can be induced by TGF- β 1, we determined the mRNA level of TGF- β 1 by using RT-PCR. As seen in Figure 5(A), TGF- β 1 mRNA was induced after 3 days of DFO stimulation, which correlated well with p27^{Kip1} expression. To confirm further whether TGF- β 1 was truly responsible for inducing p27^{Kip1} expression, p27^{Kip1} levels were examined after neutralization with anti-(TGF- β 1) antibodies. Thus Chang cells were stressed with 1 mM DFO either in the presence of 2 μ g/ml anti-(TGF- β 1) antibodies or the antibodies were added 1 day after DFO treatment. In both cases, induction of p27^{Kip1} was completely abolished by neutralization with anti-(TGF- β 1) antibodies (Figure 5B), proving that induction of p27^{Kip1} by iron chelation was mediated by TGF- β 1.

Senescence-like growth arrest by iron chelation is independent of p53

The results in Figure 3 indicated that p53 induction was most likely unrelated to the DFO-induced senescence-like growth arrest. To verify further the involvement of p53, we added DFO to the human hepatoma cell lines Huh7, which have mutant p53, and Hep3B, which lack p53. In both cell lines, DFO induced SA- β -gal activity (Figure 6A), although the intensity was weaker than in Chang cells and it took longer for the staining to be visualized, suggesting that p53 expression is not required in the DFO-induced senescence-like change. However, both p27^{Kip1} and TGF- β 1 were not induced in Hep3B cells (Figures 6B and 6C), implying that another hitherto unknown mechanism might be involved in DFO-induced senescence-like growth arrest in hepatocytes.

DISCUSSION

It is well established that iron is essential in the maintenance of cellular life, and iron overload is often found associated with cancerous cells. For the above reasons, iron deprivation has often been employed to inhibit the proliferation of malignant cells. The addition of DFO has been shown to induce growth arrest at G₁ phase in various cell lines [24,39,40], and a number of mechanisms, such as blockage of N-myc expression [23], decrease in nuclear expression of p34^{cdc2} [39] or inhibition of cyclin A protein expression [40], have been postulated. Growth arrest at G₂/M phase in certain cells, including glioma cells [41] and K562 leukaemia cells [42], has also been observed, which is dependent on dose and duration of DFO treatment. In the present study, we have demonstrated that prolonged treatment of Chang cells with a subcytotoxic concentration of DFO induced senescence-like G₁ arrest, as evidenced by reduction of growth rate, G₁ accumulation of the cells, emergence of biomarkers for replicative senescence, such as a typical flattened and enlarged morphology, SA- β -gal activity and decrease of PARP expression, and finally their irreversibility (Figure 1 and 2). To the best of our knowledge, these findings are the first to report a growth-arrest model representing replicative senescence induced by iron chelation.

On the basis of the immunoblot analysis of negative cell-cycle regulators, G₁ arrest by DFO was most likely associated with the induction of p27^{Kip1} and not the involvement of three other CDKs, p21^{Cip1}, p16^{INK4A} and p15^{INK4B} (Figure 3). p27^{Kip1} is a potent inhibitor of cyclin D/CDK4 and cyclin E/CDK2 activities, which govern cell-cycle progression at restriction and late transition points of G₁ respectively. p27^{Kip1} has been shown to be generally expressed at a high level in quiescent cells, present in a sequestered state in proliferating cells at a lower level, and rapidly down-regulated upon growth-factor stimulation [14–16]. When triggered by TGF- β 1 or contact inhibition, the role of p27^{Kip1} as a major player in G₁ arrest has been well accepted [37,38]. However, p27^{Kip1} induction by iron chelation has never been reported before, despite many studies on G₁ arrest by DFO. Our observations strongly suggested that gain of p27^{Kip1} expression by DFO could play a certain role in maintaining the growth arrest of hepatocytes at G₁ phase by DFO with acquisition of senescence-like phenotype. This suggestion is in agreement with a recent report [19] showing that senescence-like growth arrest by the phosphoinositide 3-kinase inhibitor LY294002 was mediated by p27^{Kip1}, whereas p16^{INK4A}, p21^{Cip1}, p19^{ARF} and p53 were down-regulated.

As evidenced by RT-PCR for TGF- β 1 mRNA and by neutralization with antibodies against TGF- β 1 (Figure 5), TGF- β 1 induction is heavily involved in the induction of p27^{Kip1}. Neutralization of TGF- β 1 for 2 days with antibodies was sufficient to block p27^{Kip1} induction. This indicated that the TGF- β 1 induced by DFO was released from the cells and stimulated the cells again in an autocrine manner as the major inducer of p27^{Kip1} expression. Recent reports [43,44] that TGF- β 1 can induce premature senescence in human diploid fibroblasts support further the role of TGF- β 1 as a possible mediator in DFO-induced senescence-like arrest. Unfortunately, G₁-arrested cells or senescent phenotype, such as cells having SA- β -gal activity, could not be reversed after neutralization with 3 μ g/ml anti-(TGF- β 1) antibody for 3 days as analysed by FACS and microscopic observation (results not shown). These results indicate that blocking of TGF- β 1/p27^{Kip1} signalling is not sufficient to reverse the G₁ arrest and gain of SA- β -gal activity, suggesting that other mechanisms might be involved in the arrest. The existence of another possible signalling pathway was also suggested by the observation with DFO-treated Hep3B hepatoma cells, where no TGF- β 1 and p27^{Kip1} were induced despite acquisition of the senescent phenotype (Figure 6). One possible explanation for the reason of why blocking the TGF- β 1/p27^{Kip1} induction could not reverse the arrest is that iron chelation by DFO inhibited RR, which is required for DNA synthesis, resulting in blockage of the cell-cycle progression from G₁ to S-phase [42]. There is no doubt that the RR activity cannot be recovered by the neutralization of TGF- β 1. This explanation can be supported further by recent reports [45,46] that inhibition of RR by hydroxyurea induced senescence-like growth arrest in human diploid fibroblasts and erythroleukaemia cells. In addition, we observed that DFO induced early irreversible mitochondrial dysfunction, implying that it might be involved in DFO-induced senescence-like G₁ arrest (Y.-S. Yoon, H. Cho, J.-H. Lee, K.-T. Lee and G. Yoon, unpublished work). However, in order to define more clearly the mechanism involved in DFO-induced senescence-like growth arrest of hepatocytes, possible involvement of other mediators should be pursued further. In addition the contribution of the induction of TGF- β 1/p27^{Kip1} signalling in our system has yet to be studied.

Another unexpected observation was that p21^{Cip1} was not induced, whereas p53 was. It is well known that p53 acts as a general mediator and p21, the downstream target of p53, also

plays an important role in replicative senescence [16–18]. Therefore it was of interest to observe that the DFO-induced p53 was non-functional in terms of p21^{Cip1} induction, although senescence-like arrest was induced by DFO. The reason for the inability of enhanced p53 to induce p21^{Cip1} could be explained by differential phosphorylation of p53 (Figure 4), a finding in agreement with a previous report [35] demonstrating that increased phosphorylation on Ser-15 by DFO, but not on Ser-20, prevented p53 from inducing p21^{Cip1} expression in human MRC5 fibroblasts. p53-independent replicative senescence has been demonstrated in a few studies using cells lacking p53 [32,33]. We also examined the effect of DFO on two different p53-negative cell lines, Huh7, human hepatoma cells harbouring mutant p53, and Hep3B cells, lacking p53. In both cell lines, DFO induced SA- β -gal activity (Figure 6A), suggesting that the DFO-induced senescence-like change did not require p53 expression.

In conclusion, iron chelation by DFO can inhibit cellular proliferation, especially of hepatocyte cell lines, which is accompanied by senescence-like characteristics, thus expanding our understanding on the mechanisms involved in the growth inhibition of hepatocytes by iron depletion.

We thank Dr Woon Ki Paik for critical review of this manuscript. This work was supported by grant number 2001-1-20800-003-2 from the Basic Research Program of the Korea Science and Engineering Foundation.

REFERENCES

- Robbins, E. and Pederson, T. (1970) Iron: intracellular localization and possible role in cell division. *Proc. Natl. Acad. Sci. U.S.A.* **66**, 1244–1251
- Boldt, D. H. (1999) New perspectives on iron: an introduction. *Am. J. Med. Sci.* **318**, 207–212
- Oexle, H., Gnaiger, E. and Weiss, G. (1999) Iron-dependent changes in cellular energy metabolism: influence on citric acid cycle and oxidative phosphorylation. *Biochim. Biophys. Acta* **1413**, 99–107
- Nyholm, S., Mann, G. J., Johansson, A. G., Bergeron, R. J., Graslund, A. and Thelander, L. (1993) Role of ribonucleotide reductase in inhibition of mammalian cell growth by potent iron chelators. *J. Biol. Chem.* **268**, 26200–26205
- Deugnier, Y. and Turlin, B. (2001) Iron and hepatocellular carcinoma. *J. Gastroenterol. Hepatol.* **16**, 491–494
- Bonkovsky, H. L. and Lambrecht, R. W. (2000) Iron-induced liver injury. *Clin. Liver Dis.* **4**, 409–429
- Adams, P. C. (1998) Iron overload in viral and alcoholic liver disease. *J. Hepatol.* **28**, 19–20
- Deugnier, Y., Turlin, B. and Loreal, O. (1998) Iron and neoplasia. *J. Hepatol.* **28**, 21–25
- Pietrangelo, A. (1998) Iron, oxidative stress and liver fibrogenesis. *J. Hepatol.* **28**, 8–13
- Ito, K., Mitchell, D., Gabata, T., Hann, H.-W. L., Kim, P. N., Fujita, T., Awaya, H., Honjo, K. and Matsunaga, N. (1999) Hepatocellular carcinoma association with increased iron deposition in the cirrhotic liver at MR imaging. *Radiology (Oak Brook, Ill.)* **212**, 235–240
- Hann, H.-W. L., Stahlhut, M. W. and Hann, C. L. (1990) Effect of iron and desferoxamine on cell growth and *in vitro* ferritin synthesis in human hepatoma cell lines. *Hepatology (Philadelphia)* **11**, 566–569
- Lukas, J. and Bartek, J. (2001) Pathways governing G₁/S transition and their response to DNA damage. *FEBS Lett.* **490**, 117–122
- Boonstra, J. and Hulleman, E. (2001) Regulation of G₁ phase progression by growth factors and the extracellular matrix. *Cell. Mol. Life Sci.* **58**, 80–93
- Finkel, T. and Holbrook, N. (2000) Oxidants, oxidative stress and the biology of ageing. *Nature (London)* **408**, 239–247
- Reddel, R. R. (2000) The role of senescence and immortalization in carcinogenesis. *Carcinogenesis* **21**, 477–484
- Chen, Q. M., Liu, J. and Merrett, J. B. (2000) Apoptosis or senescence-like growth arrest: influence of cell-cycle position, p53, p21 and bax in H₂O₂ response of normal human fibroblasts. *Biochem. J.* **347**, 543–551
- Vogt, M., Haggblom, C., Yeargin, J., Christiansen-Weber, T. and Haas, M. (1998) Independent induction of senescence by p16^{INK4a} and p21^{Cip1} in spontaneously immortalized human fibroblasts. *Cell Growth Differ.* **9**, 139–146
- McConnell, B. B., Starborg, M., Brookes, S. and Peters, G. (1998) Inhibitors of cyclin-dependent kinases induce features of replicative senescence in early passage human diploid fibroblasts. *Curr. Biol.* **8**, 51–354
- Collado, M., Medema, R. H., Garcia-Cao, I., Dubuisson, M. L. N., Barradas, M., Glassford, J., Rivas, C., Burgering, B. M. T., Serrano, M. and Lam, E. W.-F. (2000) Inhibition of the phosphoinositide 3-kinase pathway induces a senescence-like arrest mediated by p27^{Kip1}. *J. Biol. Chem.* **275**, 21960–21968
- Erickson, S., Sangfelt, O., Heyman, M., Castro, J., Einhorn, S. and Grandér, D. (1998) Involvement of the Ink4 proteins p16 and p15 in T-lymphocyte senescence. *Oncogene* **17**, 595–602
- Kontoghiorghes, G. J., Piga, A. and Hoffbrand, A. V. (1986) Cytotoxic and DNA-inhibitory effects of iron chelators on human leukaemic cells. *Hematol. Oncol.* **4**, 195–204
- Lederman, H. M., Cohen, A., Lee, J. W., Freedman, M. H. and Gelfand, E. W. (1984) Deferoxamine: a reversible S-phase inhibitor of human lymphocyte proliferation. *Blood* **64**, 748–753
- Fan, L., Iyer, J., Zhu, S., Frick, K. K., Wada, R. K., Eskenazi, A. E., Berg, P. E., Ikegaki, N., Kennett, R. H. and Frantz, C. N. (2001) Inhibition of N-myc expression and induction of apoptosis by iron chelation in human neuroblastoma cells. *Cancer Res.* **61**, 1073–1079
- Brodie, C., Siriwardana, G., Lucas, J., Schleicher, R., Terada, N., Szepesi, A., Gelfand, E. and Seligman, P. (1993) Neuroblastoma sensitivity to growth inhibition by deferrioxamine: evidence for a block in G₁ phase of the cell cycle. *Cancer Res.* **53**, 3968–3975
- Sakaïda, I., Hironaka, K., Uchida, K. and Okita, K. (1999) Iron chelator deferrioxamine reduces preneoplastic lesions in liver induced by choline-deficient L-amino acid-defined diet in rats. *Dig. Dis. Sci.* **44**, 560–569
- Hann, H.-W. L., Stahlhut, M. W., Rubin, R. and Maddrey, W. C. (1992) Antitumor effect of deferrioxamine on human hepatocellular carcinoma growing in athymic nude mice. *Cancer (N.Y.)* **70**, 2051–2056
- Dimri, G. P., Lee, X., Basile, G., Acosta, M., Scott, G., Roskelley, C., Medrano, E. E., Linskens, M., Rubelj, I., Pereira-Smith, O. et al. (1995) A biomarker that identifies senescent human cells in culture and in aging skin *in vivo*. *Proc. Natl. Acad. Sci. U.S.A.* **92**, 9363–9367
- Sambrook, J. and Russell, D. W. (2001) Purification of RNA from cells and tissues by acid phenol-guanidium thiocyanate-chloroform extraction. In *Molecular Cloning*, 3rd edn., pp. 7.4–7.8, Cold Spring Harbor Press, Cold Spring Harbor, NY
- Burkle, A. (1998) Poly(ADP-ribose) polymerase and aging. *Exp. Gerontol.* **33**, 519–523
- Anderson, L. E. and Dell'orco, R. T. (1991) Decline of poly(ADP-ribose)ylation during *in vitro* senescence in human diploid fibroblasts. *J. Cell. Physiol.* **146**, 216–221
- Salminen, A., Helenius, M., Lahtinen, T., Korhonen, P., Tapiola, T., Soininen, H. and Solovyan, V. (1997) Down-regulation of Ku autoantigen, DNA-dependent protein kinase, and poly(ADP-ribose) polymerase during cellular senescence. *Biochem. Biophys. Res. Commun.* **238**, 712–716
- Sugrue, M. M., Shin, D. Y., Lee, S. W. and Aaronson, S. A. (1997) Wild-type p53 triggers a rapid senescence program in human tumor cells lacking functional p53. *Proc. Natl. Acad. Sci. U.S.A.* **94**, 9648–9653
- Xiao, H., Hasegawa, T., Miyaishi, O., Ohkusu, K. and Isobe, K.-i. (1997) Sodium butyrate induces NIH3T3 cells to senescence-like state and enhances promoter activity of p21^{WAF1/Cip1} in p53-independent manner. *Biochem. Biophys. Res. Commun.* **237**, 457–460
- Caspari, T. (2000) How to activate p53. *Curr. Biol.* **10**, R315–R317
- Ashcroft, M., Taya, Y. and Vousden, K. H. (2000) Stress signals utilize multiple pathways to stabilize p53. *Mol. Cell. Biol.* **20**, 3224–3233
- Unger, T., Juven-Gershon, T., Moallem, E., Berger, M., Sionov, R. V., Lozano, G., Oren, M. and Haupt, Y. (1999) Critical role for Ser20 of human p53 in the negative regulation of p53 by Mdm2. *EMBO J.* **18**, 1805–1814
- Polyak, K., Kato, J.-V., Solomon, M., Sherr, C. J., Massague, J., Robert, J. M. and Koff, A. (1994) p27^{Kip1} and cyclin D-cdk4, interacting regulators of cdk2, link TGF- β and contact inhibition to cell cycle arrest. *Genes Dev.* **8**, 9–22
- Reynisdottir, I., Polyak, K., Iavarone, A. and Massague, J. (1995) Kip/Cip and Ink4 Cdk inhibitors cooperate to induce cell cycle arrest in response to TGF- β . *Genes Dev.* **9**, 1831–1845
- Chenoufi, N., Baffet, G., Drenou, B., Cariou, S., Desille, M., Clement, B., Brissot, P., Lescoat, G. and Loreal, O. (1998) Deferrioxamine arrests *in vitro* the proliferation of porcine hepatocyte in G₁ phase of the cell cycle. *Liver (Copenhagen)* **18**, 60–66
- Lucas, J. J., Szepesi, A., Domenico, J., Takase, K., Tordai, A., Terada, N. and Gelfand, E. W. (1995) Effects of iron-depletion on cell cycle progression in normal human T lymphocytes: selective inhibition of the appearance of the cyclin A-associated component of the p33cdk2 kinase. *Blood* **86**, 2268–2280

- 41 Renton, F. J. and Jeitner, T. M. (1996) Cell cycle-dependent inhibition of the proliferation of human neural tumor cell lines by iron chelators. *Biochem. Pharmacol.* **51**, 1553–1561
- 42 Hoyes, K. P., Hider, R. C. and Porter, J. B. (1992) Cell cycle synchronization and growth inhibition by 3-hydroxypyridin-4-one iron chelators in leukemia cell lines. *Cancer Res.* **52**, 4591–4599
- 43 Frippiat, C., Chen, Q. M., Zdanov, S., Magalhaes, J.-P., Remacle, J. and Toussaint, O. (2001) Subcytotoxic H_2O_2 stress triggers a release of transforming growth factor- β_1 , which induces biomarkers of cellular senescence of human diploid fibroblasts. *J. Biol. Chem.* **276**, 2531–2537
- 44 Katakura, Y., Nakata, E., Miura, T. and Shirahata, S. (1999) Transforming growth factor β triggers two independent-senescence programs in cancer cells. *Biochem. Biophys. Res. Commun.* **55**, 110–115
- 45 Yeo, E. J., Hwang, Y. C., Kang, C. M., Kim, I. H., Kim, D. I., Parka, J. S., Choy, H. E., Park, W. Y. and Park, S. C. (2000) Senescence-like changes induced by hydroxyurea in human diploid fibroblasts. *Exp. Gerontol.* **35**, 553–571
- 46 Park, J. I., Jeong, J. S., Han, J. Y., Kim, D. I., Gao, Y. H., Park, S. C., Rodgers, G. P. and Kim, I. H. (2000) Hydroxyurea induces a senescence-like change of K562 human erythroleukemia cell. *J. Cancer Res. Clin. Oncol.* **126**, 455–460

Received 8 October 2001/6 March 2002; accepted 11 April 2002

Published as BJ Immediate Publication 11 April 2002, DOI 10.1042/BJ20011445